SCIENTIFIC REPORTS

OPEN

Spectral features of the tunneling-induced transparency and the Autler-Townes doublet and triplet in a triple quantum dot

Xiao-Qing Luo[1], Zeng-Zhao Li[1], Jun Jing[2], Wei Xiong[1], Tie-Fu Li[1,3] & Ting Yu[1,4]

We theoretically investigate the spectral features of tunneling-induced transparency (TIT) and Autler-Townes (AT) doublet and triplet in a triple-quantum-dot system. By analyzing the eigenenergy spectrum of the system Hamiltonian, we can discriminate TIT and double TIT from AT doublet and triplet, respectively. For the resonant case, the presence of the TIT does not exhibit distinguishable anticrossing in the eigenenergy spectrum in the weak-tunneling regime, while the occurrence of double anticrossings in the strong-tunneling regime shows that the TIT evolves to the AT doublet. For the off-resonance case, the appearance of a new detuning-dependent dip in the absorption spectrum leads to double TIT behavior in the weak-tunneling regime due to no distinguished anticrossing occurring in the eigenenergy spectrum. However, in the strong-tunneling regime, a new detuning-dependent dip in the absorption spectrum results in AT triplet owing to the presence of triple anticrossings in the eigenenergy spectrum. Our results can be applied to quantum measurement and quantum-optics devices in solid systems.

Quantum coherence and interference effects can lead to considerably interesting phenomena of quantum optics such as lasing without inversion[1,2], coherent population trapping[3], correlated spontaneous emission[4], and electromagnetically induced transparency (EIT)[5–9]. As a phenomenon closely related to EIT, Autler-Townes (AT) splitting[10,11] is indicated by a *level anticrossing* in the eigenenergy spectrum and a transparency window owing to the AT doublet rather than the quantum interference. This phenomenon has been utilized to measure the state of the electromagnetic field[12–14], as well as the AT triplet and multiplet spectroscopy[15]. Both EIT and AT splitting have been investigated theoretically and experimentally in different quantum systems, including atomic and molecular systems[8,16,17], solid-state and metamaterials systems[18,19], superconducting quantum circuits[20–26] and whispering-gallery-mode optical resonators[27–29]. It is also interesting to investigate EIT and AT splitting in semiconductor nanostructures because the trapped carriers behave like atoms and can be conveniently manipulated via external fields.

In the semiconductor quantum dot (QD), excitons form bound states and play an important role in the optical properties of these systems[10,30–35]. Moreover, tunneling-induced transparency (TIT)[36–38] can occur for the excitonic states, which is similar to EIT in a three-level atomic system, but no pump field is needed to apply to the excitonic system. As shown by Borges *et al.*[37], there is an evidence regarding the coexistence of both TIT and AT doublet in the intermediate regime, when the tunneling coupling is slightly above a threshold in a double-QD system. However, a triple-QD system can offer new possibilities to study intriguing phenomena that are not observed in single and double-QD systems[39–41]. In the present paper, we show that when the electron is resonant-tunneling in such a triple-QD system, which is in contrast to the case considered in a double-QD system, the coexistence of both TIT and AT doublet regime does not occur in this system and the threshold of the tunneling coupling just corresponds to a transition point. More specifically, we find that, by analyzing the eigenenergy spectrum of the

[1]Beijing Computational Science Research Center, Beijing, 100193, China. [2]Department of Physics, Zhejiang University, Hangzhou, 310027, Zhejiang, China. [3]Institute of Microelectronics, Department of Microelectronics and Nanoelectronics and Tsinghua National Laboratory of Information Science and Technology, Tsinghua University, Beijing, 100084, China. [4]Department of Physics and Engineering Physics, Center for Controlled Quantum Systems, Stevens Institute of Technology, Hoboken, New Jersey, 07030, USA. Correspondence and requests for materials should be addressed to Z.-Z.L. (email: zengzhaoli09@gmail.com) or T.-F.L. (email: litf@tsinghua.edu.cn)
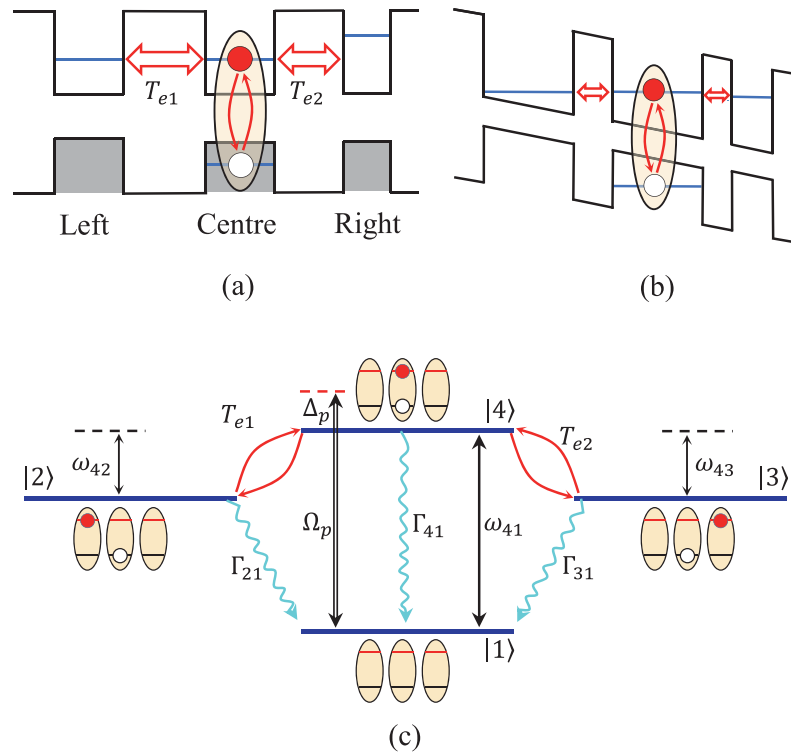
Figure 1. The coupled triple QD system. (**a**) Schematic energy-level diagram of a triple QD system without a gate voltage. (**b**) With an applied gate voltage, the energy-level in the conduction-band could get into resonance in the triple QD system. (**c**) Excitation scheme of the triple QD system, as determined by the Rabi frequency Ω_p (which is proportional to the probe-field strength), decoherence channels Γ_{m1} ($m = 2, 3, 4$), energy-level difference ω_{4n} ($n = 1, 2, 3$), probe-field detuning $\Delta_p = \omega_p - \omega_{41}$ from the energy-level difference ω_{41}, and tunneling coupling T_{ek} ($k = 1, 2$). Driven by a pulsed laser field, one electron can be excited from the valence band to the conduction band to form a direct exciton state $|4\rangle$ inside the central dot. The gate electric field allows the electron to tunnel from the central dot to the left (right) dot to form an indirect excitonic states $|2\rangle$ ($|3\rangle$). Here $|1\rangle$ denotes the state with no exciton inside this triple QD.

system Hamiltonian, there exist degenerate points in the eigenenergy spectrum for the resonant tunneling case. Therein the TIT presents in the weak-tunneling regime without displaying well-resolved anticrossing in eigenenergy spectrum. However, in the strong-tunneling regime, the *double anticrossings* in the eigenenergy spectrum illustrate the emergence of the AT doublet. For the off-resonance case, i.e., only the right dot is not resonant with the central dot, we show that the degenerate points are absent in the eigenenergy spectrum. The double TIT can be realized in the weak-tunneling regime along with the undistinguishable anticrossing in the eigenenergy spectrum and a new detuning-dependent transparency dip in the absorption spectrum. However, in the strong-tunneling regime, the presence of *triple anticrossings* in the eigenenergy spectrum reveals the realization of AT triplet in the absorption spectrum, where a new red-shifted (blue-shifted) transparency dip in the absorption spectrum is due to the presence of the blue (red) detuning from the right dot.

Results

The model.   We study a triple-QD artificial molecule consisting of three aligned QD separated by two barriers [see Fig. 1(a)]. For the purpose of inhibiting the hole tunneling between valence bands, we here consider that the central dot is identical to the left dot but structural asymmetry with the right dot. This structural asymmetry is similar to the case shown in the double quantum dots system[36,37,42–44]. With a gate (bias) voltage being applied along the growth direction, as shown in Fig. 1(b), the conduction-band-level in the left and right dot are on-resonant with the central dot[38,42,43]. In doing so, the excitonic states are composed of mostly delocalized electron states in the triple-QD accompanied with entirely localized hole states. This triple-QD system can be achieved using, e.g., a self-assembled (In, Ga) As triple-QD fabricated on a GaAs (001) substrate by molecule beam epitaxy and *in-situ* atomic layer precise etching, corresponding to a homogeneous triple-QD along the [1$\bar{1}$0] direction[39]. The system is driven by a weak probe laser field with frequency ω_p and the Rabi frequency Ω_p corresponds to the driving strength for generating the direct excitonic state in the central dot (More specifically, the electron and hole are both in the central dot). As shown in Fig. 1(c), we assume that an electron can be excited from the valence band to the conduction band via a pulsed laser field to form a direct excitonic state (denoted as $|4\rangle$) only in the central dot, where $|1\rangle$ denotes vacuum state without excitons due to the absence of optical excitation in the triple-QD system. The gate (bias) voltage just only allow the electron to tunnel from the central dot to either left or

right dot, yielding an indirect excitonic state $|2\rangle$ or $|3\rangle$ in the interdot (i.e., the electron is in the central dot but the hole is in left or right dot at this moment). The Hamiltonian for this triple-QD system reads (we set $\hbar = 1$)

$$H = \sum_{m=1}^{4} \omega_m \sigma_{mm} - \left(\Omega_p e^{-i\omega_p t} \sigma_{41} + T_{e1}\sigma_{42} + T_{e2}\sigma_{43} + \text{H.c.} \right),$$
(1)

where $\sigma_{mn} \equiv |m\rangle\langle n|$, and $\Omega_p = \mu_{14}\mathcal{E}_p/2\hbar$ is the Rabi frequency related to the probe laser field, with μ_{14} being the electric-dipole transition matrix element between $|1\rangle$ and $|4\rangle$, and $\mathcal{E}_p$ the electric-field amplitude of the probe field. T_{e1} (T_{e2}) denotes the tunneling coupling between the central dot and the left (right) dot, which can be controlled by regulating the width of the barrier and the applied gate voltage between the central dot and the left (right) dot.

Using a unitary transformation $U(t) = \exp\left[-i\omega_p(\sum_{m=2}^{4}\sigma_{mm})t\right]$ to remove the time-dependent oscillatory terms[24], we can write the Hamiltonian in the interaction picture as

$$H_I = -\Delta_p \sigma_{44} - \Delta_2 \sigma_{22} - \Delta_3 \sigma_{33} - (\Omega_p \sigma_{41} + T_{e1}\sigma_{42} + T_{e2}\sigma_{43} + \text{H.c.}),$$
(2)

with $\Delta_p = \omega_p - \omega_{41}$, $\Delta_2 = \Delta_p + \omega_{42}$, and $\Delta_3 = \Delta_p + \omega_{43}$. Here Δ_p denotes the detuning of the probe field from ω_{41}, and $\omega_{4n}(n = 2, 3)$ is the energy difference between $|4\rangle$ and $|n\rangle$. For the triple-QD system described by Hamiltonian (2), when $\Delta_p = 0$, the system has the degenerate dark states $|\psi_1\rangle_{\text{dark}}$ and $|\psi_2\rangle_{\text{dark}}$ as follows

$$|\psi_1\rangle_{\text{dark}} = \cos\theta|3\rangle - \sin\theta|1\rangle,$$
(3a)

$$|\psi_2\rangle_{\text{dark}} = \cos\theta\sin\phi|1\rangle + \sin\theta\sin\phi|3\rangle - \cos\phi|2\rangle,$$
(3b)

where

$$\tan\theta = \frac{T_{e2}}{\Omega_p}, \quad \tan\phi = \frac{T_{e1}}{\sqrt{\Omega_p^2 + T_{e2}^2}}.$$
(4)

Note that when $T_{e2} = 0$, $|\psi_2\rangle_{\text{dark}}$ is reduced to the dark state in a Λ-type three-level QD system, $|\psi\rangle_{\text{dark}} = \sin\Theta|1\rangle - \cos\Theta|2\rangle$ with $\tan\Theta = T_{e1}/\Omega_p$.

The dynamics of the system can be described by a Lindblad master equation:

$$\frac{\partial\rho}{\partial t} = -\frac{i}{\hbar}[H_I, \rho] + \sum_{m=2}^{4}\left(\frac{\Gamma_{m1}}{2}\mathcal{D}[\sigma_{1m}]\rho + \gamma_m^\phi \mathcal{D}[\sigma_{mm}]\rho \right),$$
(5)

where $\mathcal{D}[\hat{\mathcal{O}}]\rho = 2\hat{\mathcal{O}}\rho\hat{\mathcal{O}}^\dagger - \hat{\mathcal{O}}^\dagger\hat{\mathcal{O}}\rho - \rho\hat{\mathcal{O}}^\dagger\hat{\mathcal{O}}$, Γ_{m1} are the relaxation rates between $|m\rangle$ and $|1\rangle$, and γ_m^ϕ describe the pure dephasing rates of the states $|m\rangle$ ($m = 2, 3, 4$). The decoherence of the excitonic states is induced by both spontaneous radiation and pure dephasing processes. For the explicit expression of the master equation, see Eq. (12) in Methods.

Also, as shown in Methods, the density matrix element ρ_{14} in the steady state is given by

$$\rho_{14} = \frac{d_2 d_3 \Omega_p^*}{d_2 d_3 d_4 - T_{e1}^2 d_3 - T_{e2}^2 d_2},$$
(6)

where $d_{2(3)} = \Delta_{2(3)} + i\Gamma_{2(3)}$, and $d_4 = \Delta_p + i\Gamma_4$. It can be seen that when $T_{e2} = 0$, i.e., in the absence of the right-side electron tunneling in Fig. 1, Eq. (6) is reduced to the result for the linear response of a Λ-type three-level QD system[37].

Next we decompose the density matrix element ρ_{14} into two components. In this way, ρ_{14} in Eq. (6) is decomposed as

$$\rho_{14} = R_{\text{I}} + R_{\text{II}},$$
(7a)

$$R_{\text{I}} = \frac{R_+}{\Delta_p - \Delta_+}, \quad R_{\text{II}} = \frac{R_-}{\Delta_p - \Delta_-},$$
(7b)

where

$$\Delta_\pm = \frac{1}{2}[-(\omega_{42} + i\Gamma_2 + i\Gamma_4) \pm \alpha], \quad R_\pm = \pm\frac{(\Delta_\pm + \omega_{42} + i\Gamma_2)}{\alpha},$$
(8a)

$$\alpha^2 = [\omega_{42} - i(\Gamma_4 - \Gamma_2)]^2 + 4T_{e1}^2 + 4\frac{d_2}{d_3}T_{e2}^2.$$
(8b)

The two terms R_{I} and R_{II} represent the first ("I") and second ("II") resonances, respectively. The two resonances can be directly used to analyze the characters of the probe-field absorption in our scheme[37,45].

Tunneling-induced transparency and Autler-Townes doublet.   We first consider the case of an electron resonantly tunneling in the triple-QD system, i.e., $\omega_{42} = \omega_{43} = 0$. For simplicity, let $\Gamma_2 = \Gamma_3$. Then, $d_2 = d_3$, and one can analytically solve $\alpha = 0$ in Eq. (8b) (see refs[25,29,37] and[45]). It is shown that a transition point turns out at the threshold coupling strength $T_t \cong \Gamma_4/2$. Note that in the intermediate coupling regime ($T_t < \sqrt{T_{e1}^2 + T_{e2}^2} < \Gamma_4$), in contrast to the case shown in the three-level Λ system[37], the first-resonance R_{I} and the second-resonance R_{II}, which have the same sign in absorption profile are apparently separated, indicating that there is no interference in this case. In other words, the crossover regime does not occur in this triple-QD system. Thus, there are only two regimes in such a system, i.e., the threshold T_t separates TIT in the weak-tunneling regime ($0 < \sqrt{T_{e1}^2 + T_{e2}^2} < T_t$) from AT doublet in the strong-tunneling regime ($\sqrt{T_{e1}^2 + T_{e2}^2} > T_t$).

(1) The weak-tunneling regime.   In the weak-tunneling regime with $0 < \sqrt{T_{e1}^2 + T_{e2}^2} < T_t$, α is a pure imaginary number. It gives rise to a pure real number $R_{\pm} = 1/2 \mp \varepsilon_1/|\alpha|$, with $\varepsilon_1 = (\Gamma_4 - \Gamma_2)/2$, and a pure imaginary number $\Delta_{\pm} = i(-\varepsilon_2 \pm |\alpha|/2)$, with $\varepsilon_2 = (\Gamma_4 + \Gamma_2)/2$. Thus, the imaginary part of ρ_{14} is given by

$$\mathrm{Im}(\rho_{14})_{\mathrm{TIT}} = \mathrm{Im}(R_{\mathrm{I}})_{\mathrm{TIT}} + \mathrm{Im}(R_{\mathrm{II}})_{\mathrm{TIT}}, \tag{9a}$$

$$\mathrm{Im}(R_{\mathrm{I}})_{\mathrm{TIT}} = \frac{C_{\mathrm{I}}}{\Delta_p^2 + \Delta_+^2}, \quad \mathrm{Im}(R_{\mathrm{II}})_{\mathrm{TIT}} = \frac{-C_{\mathrm{II}}}{\Delta_p^2 + \Delta_-^2}, \tag{9b}$$

where

$$C_{\mathrm{I}} = \left(\frac{1}{2} - \frac{\varepsilon_1}{|\alpha|}\right)\left(-\varepsilon_2 + \frac{|\alpha|}{2}\right), \quad C_{\mathrm{II}} = \left(\frac{1}{2} + \frac{\varepsilon_1}{|\alpha|}\right)\left(\varepsilon_2 + \frac{|\alpha|}{2}\right). \tag{10}$$

In the weak-tunneling case, $0 < |\alpha|/2 < \varepsilon_1, \varepsilon_2$, so that both the parameters C_{I} and C_{II} are positive. Then, the first-resonance term $\mathrm{Im}(R_{\mathrm{I}})_{\mathrm{TIT}}$ is a wide, positive Lorentz line profile, while the second-resonance term $\mathrm{Im}(R_{\mathrm{II}})_{\mathrm{TIT}}$ is a narrow, negative Lorentz line profile. The different signs of the first and second resonances profile indicate the realization of the TIT, as due to the destructive interference.

As shown in Fig. 2(a), when the tunneling couplings T_{e1} and T_{e2} are both weak (i.e., $T_{e1} = T_{e2} = \Gamma_4/5$), it is interesting to see that the eigenenergies of this system Hamiltonian do not display an obvious anticrossing, but show degenerate points when the electron is resonant tunneling among the triple-QD system ($\omega_{42} = \omega_{43} = 0$). However, there is an evidence of a double anticrossing in the eigenenergy spectrum of the system Hamiltonian [see the red dashed loops in Fig. 2(d)], when the relative tunneling coupling ($T_{re} = \sqrt{T_{e1}^2 + T_{e2}^2}$, with $T_{e1} = \Gamma_4/2$, $T_{e2} = 10^{-1}\Gamma_4$) is slightly stronger than the threshold coupling strength $T_t = \Gamma_4/2$. Furthermore, these results also indicate that the coexistence of both TIT and AT doublet does not occur in such a triple-QD system, and the threshold of the tunneling coupling just corresponds to a transition point.

(2) The strong-tunneling regime.   In the strong-tunneling regime with $T_t < \sqrt{T_{e1}^2 + T_{e2}^2}$, $\alpha = 2\sqrt{T_{e1}^2 + T_{e2}^2}$ is a real number, such that $R_{\pm} = 1/2$ and $\Delta_{\pm} = -i\varepsilon_2 \pm \alpha/2$. The two resonances are located at $\pm\alpha/2$ and have the same linewidth ε_2. The imaginary part of ρ_{14} in this regime can be written as

$$\mathrm{Im}(\rho_{14})_{\mathrm{ATD}} = \mathrm{Im}(R_{\mathrm{I}})_{\mathrm{ATD}} + \mathrm{Im}(R_{\mathrm{II}})_{\mathrm{ATD}}, \tag{11a}$$

$$\mathrm{Im}(R_{\mathrm{I}})_{\mathrm{ATD}} = \frac{-\varepsilon_2/2}{\left(\Delta_p - \frac{\alpha}{2}\right)^2 + \varepsilon_2^2}, \quad \mathrm{Im}(R_{\mathrm{II}})_{\mathrm{ATD}} = \frac{-\varepsilon_2/2}{\left(\Delta_p + \frac{\alpha}{2}\right)^2 + \varepsilon_2^2}. \tag{11b}$$

This corresponds to an AT doublet because of $\mathrm{Im}(\rho_{14})_{\mathrm{ATD}}$ is the sum of two identical Lorentz line profile peaked at $\pm\alpha/2$[11]. It is interesting to see that the appearance of the AT doublet in the absorption spectrum of the probe field is equivalent to the case that there exist the double anticrossings in the eigenenergies of the system Hamiltonian [as shown in the red dashed loops in Fig. 2(b)], forming a transparency window between the pair of resonances. Now the positive value of the resonance pair is only responsible for the decreasing or even vanishing absorption of the probe field, instead of accounting for this phenomenon through the cause for that of the destructive interference in the TIT[29,37]. This is because the pair of resonances is shifted relatively far away from each other, so that their overlap is insufficient to yield significant interference.

When the tunneling couplings are sufficiently strong ($T_{e1}, T_{e2} \geq \Gamma_4$), there are prominent double anticrossings in the eigenenergies of the system Hamiltonian [as shown in the red dashed loops in Fig. 2(c)]. This also gives rise to an evident reduction of the overall absorption, displaying a wide transparency window (corresponding to vanishing absorption)[37]. The pronounced double anticrossings in this situation can be used to deduce the positions and width of the transparency window of the AT doublet. Therefore, in this strong-tunneling regime, the TIT evolves to the AT doublet, which results in a well-resolved doublet in the absorption spectrum and double anticrossings in the eigenenergy spectrum.

Double Tunneling-induced transparency and Autler-Townes triplet.   Next, we consider the case of an electron resonant tunneling between the left and central dots (i.e., $\omega_{42} = 0$), while there is off-resonant tunneling between the right and central dots (that is, $\omega_{43} \neq 0$) in the triple-QD system. The energy shift induced by the gate field is given by $\Delta\omega_{43} = eFd$[38,42], with F being the fixed electric field and d being the width of the barrier
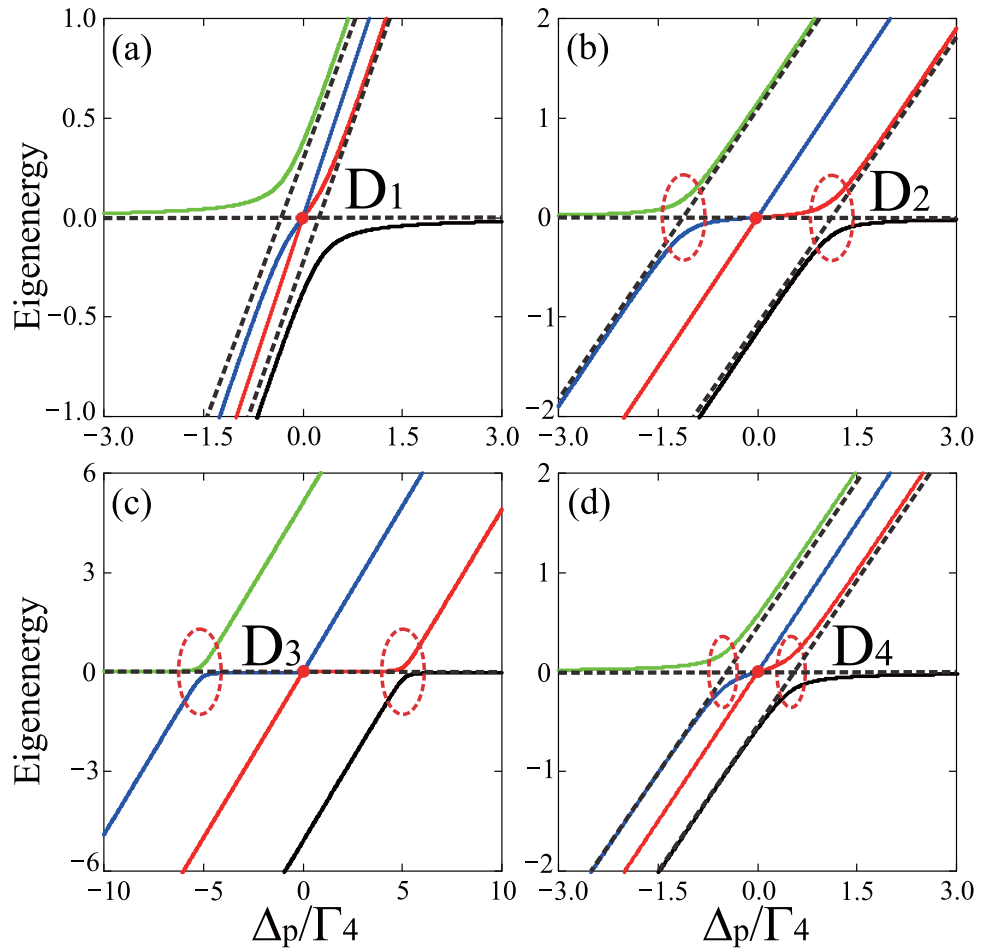
Figure 2. Eigenenergy spectrum of the system's Hamiltonian with resonant detuning. Eigenenergies of the Hamiltonian (2) as a function of the probe-field detuning Δ_p at different values of the tunneling coupling strength: (**a**) $T_{e1} = T_{e2} = \Gamma_4/5$, (**b**) $T_{e1} = \Gamma_4/2$, $T_{e2} = \Gamma_4$, (**c**) $T_{e1} = \Gamma_4$, $T_{e2} = 5\Gamma_4$, and (**d**) $T_{e1} = \Gamma_4/2$, $T_{e2} = 10^{-1}\Gamma_4$, where $\Gamma_4 = 10\,\mu eV$. Other parameters are chosen as $\Omega_p = 10^{-2}\Gamma_4$ and $\omega_{42} = \omega_{43} = 0$. Here D_i ($i = 1, 2, 3, 4$) labels the degenerate points in the eigenenergy diagrams and the red dashed loops are used to highlight the anticrossing points.

between the right and central dot. In this scenario, the optical absorption of the probe field can be manipulated by varying the fixed electric field F, which is a way of controlling the detuning of the right dot ω_{43}. It should be noted that, as shown in Fig. 3, the degenerate points of the eigenenergies of the system Hamiltonian disappear when ω_{43} is nonzero. For instance, when $\omega_{43} = \pm\Gamma_4/5$, there are not degenerate points and distinguishable anticrossing in the eigenenergies of the system Hamiltonian in the weak-tunneling regime [see Fig. 3(a)], which is clearly distinct from the results shown in a double-QD system[37]. In the strong-tunneling regime, one can also see that the eigenenergies of the system Hamiltonian exhibit triple anticrossings [see Fig. 3(b)], as compared to the case with double anticrossings being implied to denote AT doublet in Fig. 2(b) where $\omega_{43} = 0$.

(1) The weak-tunneling regime with $\omega_{43} \neq 0$. As shown in Fig. 4(a), in the weak-tunneling regime, it is revealed that double TIT can be realized by manipulating the energy-level detuning Δ_3 to achieve slight off-resonance. Narrow double transparency windows arise, when the tunneling couplings are weaker than or equal to the threshold value T'_t [as shown in Eq. (8b), there is indeed threshold value in this case but no explicit expression], in the case of $\omega_{43} \neq 0$. In particular, the new TIT dip [see the blue dashed curve in Fig. 4(a)] is red-shifted for a blue-detuned Δ_3 (e.g., $\omega_{43} = \Gamma_4/5$) in the probe field absorption spectrum. However, the new TIT dip [see the red dotted curve in Fig. 4(a)] becomes blue-shifted at a red-detuned Δ_3 (e.g., $\omega_{43} = -\Gamma_4/5$) in the absorption spectrum. Furthermore, both the undistinguished anticrossing in the eigenenergy spectrum [see Fig. 3(a)] and the new detuning-dependent dip presenting within the scope of the full-linewidth [see the black curve in Fig. 4(a)] in the absorption spectrum demonstrate that the double TIT is implemented. Hence, the double TIT is significantly different from AT doublet, where the peaks of the pair resonances are far enough separated apart and the double anticrossings occur in the eigenenergy spectrum. Moreover, as shown in Fig. 4(b), one of the absorption minima in the probe field absorption spectrum obeys the condition $\Delta_p = \omega_{42} = 0$, and the other absorption minimum
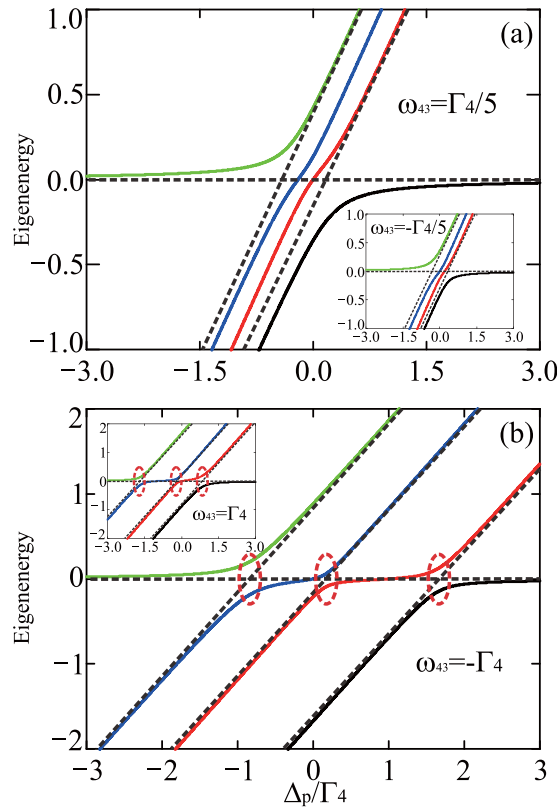
Figure 3. Eigenenergy spectrum of the system's Hamiltonian with off-resonant detuning. Eigenenergies of the Hamiltonian (2) as a function of the probe-field detuning Δ_p at different values of the tunneling couplings strength and the frequency difference ω_{43}: (**a**) $T_{e1} = T_{e2} = \Gamma_4/5$, $\omega_{43} = \pm\Gamma_4/5$, and (**b**) $T_{e2} = 2T_{e1} = \Gamma_4 = 10\,\mu eV$, $\omega_{43} = \pm\Gamma_4$, with $\omega_{42} = 0$ and $\Omega_p = 10^{-2}\Gamma_4$. The red dashed loops are used to highlight the anticrossing points.

satisfies the condition $\Delta_p = -\omega_{43}$. Therefore, we are able to realize double TIT without forming well-resolved anticrossing in such a weak-tunneling regime.

(2) The strong-tunneling regime with $\omega_{43} \neq 0$. In the strong-tunneling regime, the transparency window of the AT doublet [see the black solid curve in Fig. 4(c)] exhibits a new peak, turning the probe field absorption profile into three peaks. This yields two transparency windows [as shown in the blue dashed and red dotted curves in Fig. 4(c)], where a new dip arises in the blue (red) side of the probe detuning accompanied with the other two peaks of the transparency window being blue-shifted (red-shifted) when there is a red-detuned (blue-detuned) Δ_3, e.g., $\omega_{43} = \mp\Gamma_4/5$. Also, one can see that the triple anticrossings in the eigenenergy spectrum [see Fig. 3(b)] make sure that the AT triplet is fulfilled at this moment. In Fig. 4(d), similar features can be observed, where two absorption minima in the absorption spectrum locate at $\Delta_p = \omega_{42} = 0$ and $\Delta_p = -\omega_{43}$, respectively. It should be noted that the width of the central peak increases when raising the blue-detuning (red-detuning) Δ_3, but the width of the peak on the red-detuned (blue-detuned) side decreases. In particular, for a blue-detuned (red-detuned) Δ_3, the decrease of the width of the red-detuned (blue-detuned) sideband is compensated by the increase of the width of the central peak. Therefore, in the strong-tunneling regime, the AT triplet can be realized by manipulating the detuning Δ_3.

Discussion

In this work, we have presented a theoretical study of the eigenenergy spectrum and optical absorption properties of a triple-QD system with four effective energy levels. The results show that, in the case of the electron resonant-tunneling in the triple-QD system, there are degenerate points in the eigenenergy spectrum of the system Hamiltonian. In the weak-tunneling regime, the presence of the TIT does not show an obvious anticrossing in the eigenenergy spectrum. However, in the strong-tunneling regime, the emergence of double anticrossings in the eigenenergy spectrum indicates that the TIT evolves to the AT doublet which includes two well-resolved peaks in the probe field absorption spectrum. The pronounced double anticrossings in the eigenenergy spectrum of the system Hamiltonian that can be used to deduce the positions and width of the transparency window of the AT doublet. For the off-resonance case, that is, the right dot is not resonant with the central dot, we demonstrate that the degenerate points in the eigenenergy spectrum disappear. The realization of double TIT in the weak-tunneling regime, where the distinguishable anticrossing does not appear in the eigenenergy spectrum, exhibits a new transparency dip in the absorption spectrum which can be controlled by manipulating one of the energy-level detunings. However, in the strong-tunneling regime, the presence of triple anticrossings in the eigenenergy spectrum illustrates the realization of AT triplet in the absorption spectrum. More importantly,
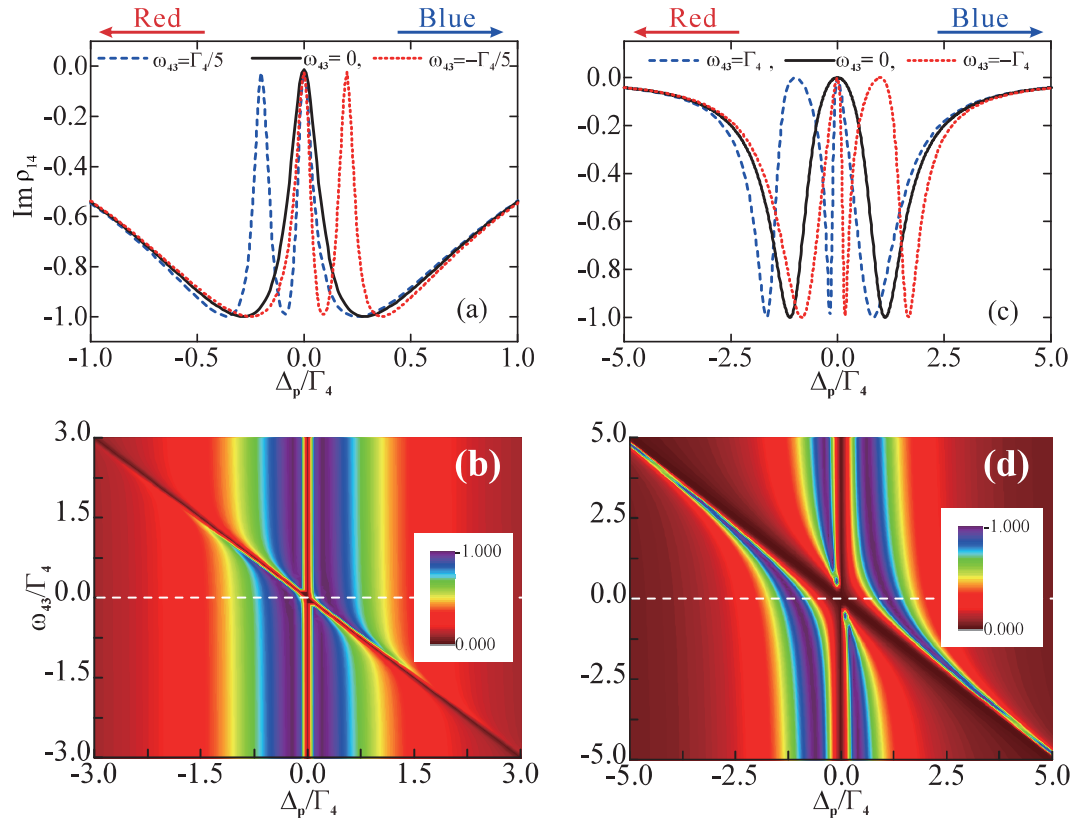
Figure 4. Double Tunneling-induced transparency and Autler-Townes triplet. (**a,b**) Im(ρ_{14}) as a function of the probe-field detuning Δ_p at different values of the frequency difference ω_{43}, where $T_{e1} = T_{e2} = \Gamma_4/5$; (**c,d**) Im($\rho_{14}$) as a function of both the probe-field detuning Δ_p and the frequency difference ω_{43}, where $T_{e2} = 2T_{e1} = \Gamma_4 = 10\,\mu eV$. Here $\omega_{42} = 0$ and $\Gamma_2 = \Gamma_3 = 10^{-3}\Gamma_4$.

there is a new dip in the blue (red) side of the probe detuning along with the other two peaks of the transparency window being blue-shifted (red-shifted) at a red-detuned (blue-detuned) Δ_3. The linewidth narrowing in one of the side peaks could be compensated for the linewidth broadening in the central peak.

Finally, our proposed schemes for these spectral features are naturally inherited and open up new ways for physicists and chemists to work in the field of laser spectroscopy, quantum measurement, nonlinear optics and quantum-optics devices in solid systems.

Methods

Quantum dynamics behavior of the triple QD system. By applying the Born-Markov approximation, the coupled differential equations for the density matrix ρ_{mn} in the interaction picture can be obtained as

$$
\begin{aligned}
\partial_t\rho_{11} &= \Gamma_{21}\rho_{22} + \Gamma_{31}\rho_{33} + \Gamma_{41}\rho_{44} - i\Omega_p\rho_{14} + i\Omega_p^*\rho_{41}, \\
\partial_t\rho_{22} &= -\Gamma_{21}\rho_{22} - iT_{e1}\rho_{24} + iT_{e1}\rho_{42}, \\
\partial_t\rho_{33} &= -\Gamma_{31}\rho_{33} - iT_{e2}\rho_{34} + iT_{e2}\rho_{43}, \\
\partial_t\rho_{44} &= -\Gamma_{41}\rho_{44} + i\Omega_p^*\rho_{14} + iT_{e1}\rho_{24} + iT_{e2}\rho_{34} \\
&\quad -i\Omega_p\rho_{41} - iT_{e1}\rho_{42} - iT_{e2}\rho_{43}, \\
\partial_t\rho_{12} &= i(\Delta_2 + i\Gamma_2)\rho_{12} - iT_{e1}\rho_{14} + i\Omega_p^*\rho_{42}, \\
\partial_t\rho_{13} &= i(\Delta_3 + i\Gamma_3)\rho_{13} - iT_{e2}\rho_{14} + i\Omega_p^*\rho_{43}, \\
\partial_t\rho_{14} &= i(\Delta_p + i\Gamma_4)\rho_{14} - iT_{e1}\rho_{12} - iT_{e2}\rho_{13} \\
&\quad -i\Omega_p^*(\rho_{11} - \rho_{44}), \\
\partial_t\rho_{23} &= i(\Delta_3 - \Delta_2 + i\gamma_{23})\rho_{23} - iT_{e2}\rho_{24} + iT_{e1}\rho_{43}, \\
\partial_t\rho_{24} &= i(\Delta_p - \Delta_2 + i\gamma_{24})\rho_{24} - i\Omega_p^*\rho_{21} - iT_{e2}\rho_{23} \\
&\quad -iT_{e1}(\rho_{22} - \rho_{44}), \\
\partial_t\rho_{34} &= i(\Delta_p - \Delta_3 + i\gamma_{34})\rho_{34} - i\Omega_p^*\rho_{31} - iT_{e1}\rho_{32} \\
&\quad -iT_{e2}(\rho_{33} - \rho_{44}),
\end{aligned}
\tag{12}
$$

with $\Gamma_m = \Gamma_{m1}/2 + \gamma_m^\phi$ ($m = 2, 3$ and 4), and $\gamma_{mn} = (\Gamma_{m1} + \Gamma_{n1})/2 + \gamma_m^\phi + \gamma_n^\phi$ ($m = 2, 3; n = 3, 4$).

The derivation of the solution of the density matrix ρ_{14}. From Eq. (12), when the time is explicitly shown in the equations of $\partial_t \rho_{12}$, $\partial_t \rho_{13}$, and $\partial_t \rho_{14}$, it follows that

$$
\begin{aligned}
\partial_t \rho_{12}(t) &= i(\Delta_2 + i\Gamma_2)\rho_{12}(t) - iT_{e1}\rho_{14}(t) + i\Omega_p^* \rho_{42}(t), \\
\partial_t \rho_{13}(t) &= i(\Delta_3 + i\Gamma_3)\rho_{13}(t) - iT_{e2}\rho_{14}(t) + i\Omega_p^* \rho_{43}(t), \\
\partial_t \rho_{14}(t) &= i(\Delta_p + i\Gamma_4)\rho_{14}(t) - iT_{e1}\rho_{12} - iT_{e2}\rho_{13}(t) \\
&\quad - i\Omega_p^*(\rho_{11}(t) - \rho_{44}(t)).
\end{aligned}
\tag{13}
$$

The absorption and dispersion coefficients are respectively proportional to the imaginary and real parts of the density matrix element ρ_{14} in the steady state[37,45]. With a weak probe field ($\Omega_p \ll T_{e1}, T_{e2}$) acting on the considered triple-QD system, the term $\Omega_p^* \rho_{42}(t)$ and $\Omega_p^* \rho_{43}(t)$ in Eq. (13) can be respectively approximated by $\Omega_p^* \rho_{42}(0)$ and $\Omega_p^* \rho_{43}(0)$, and the term $\Omega_p^*[\rho_{11}(t) - \rho_{44}(t)]$ can also be approximated by $\Omega_p^*[\rho_{11}(0) - \rho_{44}(0)]$. Moreover, the system is assumed to be initially in the ground state $|1\rangle$, so $\rho_{11}(0) = 1$ and $\rho_{42}(0) = \rho_{43}(0) = \rho_{44}(0) = 0$. Then, Eq. (13) becomes

$$
\begin{aligned}
\partial_t \rho_{12} &= i(\Delta_2 + i\Gamma_2)\rho_{12} - iT_{e1}\rho_{14}, \\
\partial_t \rho_{13} &= i(\Delta_3 + i\Gamma_3)\rho_{13} - iT_{e2}\rho_{14}, \\
\partial_t \rho_{14} &= i(\Delta_p + i\Gamma_4)\rho_{14} - iT_{e1}\rho_{12} - iT_{e2}\rho_{13} - i\Omega_p^*.
\end{aligned}
\tag{14}
$$

In the steady-state, $\partial_t \rho_{12} = \partial_t \rho_{13} = \partial_t \rho_{14} = 0$, so we have

$$
\rho_{14} = \frac{d_2 d_3 \Omega_p^*}{d_2 d_3 d_4 - T_{e1}^2 d_3 - T_{e2}^2 d_2}.
\tag{15}
$$

References

1. Harris, S. E. Lasers without inversion: Interference of lifetime-broadened resonances. *Phys. Rev. Lett.* **62**, 1033–1036 (1989).
2. Scully, M. O., Zhu, S.-Y. & Gavrielides, A. Degenerate quantum-beat laser: Lasing without inversion and inversion without lasing. *Phys. Rev. Lett.* **62**, 2813–2816 (1989).
3. Arimondo, E. Coherent population trapping in laser spectroscopy. *Prog. Opt.* **35**, 257–354 (1996).
4. Scully, M. O. Correlated spontaneous-emission lasers: Quenching of quantum fluctuations in the relative phase angle. *Phys. Rev. Lett.* **55**, 2802–2805 (1985).
5. Harris, S. E. Electromagnetically induced transparency. *Phys. Today* **50**, 36–42 (1997).
6. Fleischhauer, M., Imamoğlu, A. & Marangos, J. P. Electromagnetically induced transparency: Optics in coherent media. *Rev. Mod. Phys.* **77**, 633–673 (2005).
7. Marangos, J. P. Electromagnetically induced transparency. *J. Mod. Opt.* **45**, 471–503 (1998).
8. Hau, L. V., Harris, S. E., Dutton, Z. & Behroozi, C. H. Light speed reduction to 17 meters per second in an ultracold atomic gas. *Nature* **397**, 594–598 (1999).
9. Schmidt, H. & Imamoğlu, A. Giant Kerr nonlinearities obtained by electromagnetically induced transparency. *Opt. Lett.* **21**, 1936–1938 (1996).
10. Autler, S. H. & Townes, C. H. Stark effect in rapidly varying fields. *Phys. Rev.* **100**, 703–722 (1955).
11. Cohen-Tannoudji, C. N. *The Autler-Townes effect revisited* (Springer, 1996).
12. Zubairy, M. S. Quantum state measurement via Autler-Townes spectroscopy. *Phys. Lett. A* **222**, 91–96 (1996).
13. Herkommer, A., Schleich, W. & Zubairy, M. Autler-Townes microscopy on a single atom. *J. Mod. Opt.* **44**, 2507–2513 (1997).
14. Ikram, M. & Zubairy, M. S. Reconstruction of an entangled state in a cavity via Autler-Townes spectroscopy. *Phys. Rev. A* **65**, 044305 (2002).
15. Ghafoor, F. Autler-Townes multiplet spectroscopy. *Laser Phys.* **24**, 035702 (2014).
16. Lukin, M. *et al.* Spectroscopy in dense coherent media: Line narrowing and interference effects. *Phys. Rev. Lett.* **79**, 2959–2962 (1997).
17. Mücke, M. *et al.* Electromagnetically induced transparency with single atoms in a cavity. *Nature* **465**, 755–758 (2010).
18. Zhang, S., Genov, D. A., Wang, Y., Liu, M. & Zhang, X. Plasmon-induced transparency in metamaterials. *Phys. Rev. Lett.* **101**, 047401 (2008).
19. Liu, N. *et al.* Plasmonic analogue of electromagnetically induced transparency at the Drude damping limit. *Nat. Mater.* **8**, 758–762 (2009).
20. Alzar, C. G., Martinez, M. & Nussenzveig, P. Classical analog of electromagnetically induced transparency. *Am. J. Phys.* **70**, 37–41 (2002).
21. Abdumalikov, A. Jr. *et al.* Electromagnetically induced transparency on a single artificial atom. *Phys. Rev. Lett.* **104**, 193601 (2010).
22. Anisimov, P. M., Dowling, J. P. & Sanders, B. C. Objectively discerning Autler-Townes splitting from electromagnetically induced transparency. *Phys. Rev. Lett.* **107**, 163604 (2011).
23. You, J. & Nori, F. Atomic physics and quantum optics using superconducting circuits. *Nature* **474**, 589–597 (2011).
24. Xiang, Z.-L., Ashhab, S., You, J. & Nori, F. Hybrid quantum circuits: Superconducting circuits interacting with other quantum systems. *Rev. Mod. Phys.* **85**, 623–653 (2013).
25. Sun, H.-C. *et al.* Electromagnetically induced transparency and Autler-Townes splitting in superconducting flux quantum circuits. *Phys. Rev. A* **89**, 063822 (2014).
26. Liu, Q.-C. *et al.* Method for identifying electromagnetically induced transparency in a tunable circuit quantum electrodynamics system. *Phys. Rev. A* **93**, 053838 (2016).
27. Xu, Q. *et al.* Experimental realization of an on-chip all-optical analogue to electromagnetically induced transparency. *Phys. Rev. Lett.* **96**, 123901 (2006).
28. Totsuka, K., Kobayashi, N. & Tomita, M. Slow light in coupled-resonator-induced transparency. *Phys. Rev. Lett.* **98**, 213904 (2007).
29. Peng, B., Özdemir, Ş. K., Chen, W., Nori, F. & Yang, L. What is and what is not electromagnetically induced transparency in whispering-gallery microcavities. *Nat. Commun* **5**, 5082 (2014).

30. Knox, R. S. *Theory of excitons* (Academic Press, 1963).
31. Brunner, K., Abstreiter, G., Böhm, G., Tränkle, G. & Weimann, G. Sharp-line photoluminescence and two-photon absorption of zero-dimensional biexcitons in a GaAs/AlGaAs structure. *Phys. Rev. Lett.* **73**, 1138–1141 (1994).
32. Jundt, G., Robledo, L., Högele, A., Fält, S. & Imamoğlu, A. Observation of dressed excitonic states in a single quantum dot. *Phys. Rev. Lett.* **100**, 177401 (2008).
33. Gerardot, B. *et al*. Dressed excitonic states and quantum interference in a three-level quantum dot ladder system. *New J. Phys* **11**, 013028 (2009).
34. Li, X. *et al*. An all-optical quantum gate in a semiconductor quantum dot. *Science* **301**, 809–811 (2003).
35. Akopian, N. *et al*. Entangled photon pairs from semiconductor quantum dots. *Phys. Rev. Lett.* **96**, 130501 (2006).
36. Berney, J., Portella-Oberli, M. T. & Deveaud, B. Dressed excitons within an incoherent electron gas: Observation of a mollow triplet and an Autler-Townes doublet. *Phys. Rev. B* **77**, 121301 (2008).
37. Borges, H., Sanz, L., Villas-Bôas, J., Neto, O. D. & Alcalde, A. Tunneling induced transparency and slow light in quantum dot molecules. *Phys. Rev. B* **85**, 115425 (2012).
38. Borges, H., Sanz, L., Villas-Bôas, J. & Alcalde, A. Quantum interference and control of the optical response in quantum dot molecules. *Appl. Phys. Lett.* **103**, 222101 (2013).
39. Hsieh, C.-Y., Shim, Y.-P., Korkusinski, M. & Hawrylak, P. Physics of lateral triple quantum-dot molecules with controlled electron numbers. *Rep. Prog. Phys.* **75**, 114501 (2012).
40. Saraga, D. S. & Loss, D. Spin-entangled currents created by a triple quantum dot. *Phys. Rev. Lett.* **90**, 166803 (2003).
41. Grove-Rasmussen, K., Jørgensen, H. I., Hayashi, T., Lindelof, P. E. & Fujisawa, T. A triple quantum dot in a single-wall carbon nanotube. *Nano. Lett.* **8**, 1055–1060 (2008).
42. Bracker, A. S. *et al*. Engineering electron and hole tunneling with asymmetric InAs quantum dot molecules. *Appl. Phys. Lett.* **89**, 233110 (2006).
43. Villas-Bôas, J. M., Govorov, A. O. & Ulloa, S. E. Coherent control of tunneling in a quantum dot molecule. *Physical Review B* **69**, 125342 (2004).
44. Borges, H., Alcalde, A. & Ulloa, S. E. Exchange interaction and tunneling-induced transparency in coupled quantum dots. *Phys. Rev. B* **90**, 205311 (2014).
45. Abi-Salloum, T. Y., Henry, B., Davis, J. P. & Narducci, F. A. Resonances and excitation pathways in four-level N-scheme atomic systems. *Phys. Rev. A* **82**, 013834 (2010).

Acknowledgements

Author Contributions

All authors have made substantial intellectual contributions to the research work. X.Q.L. performed the calculations, and Z.Z.L. also participated in the discussions. All authors contributed to the interpretation of the work and the writing of the manuscript.

Additional Information

Competing Interests: The authors declare no competing interests.

Publisher's note: Springer Nature remains neutral with regard to jurisdictional claims in published maps and institutional affiliations.